AIP Advances

Ultrafast charge migration in ionized iodo-alkyne chain $I(CC)_nH^+$

Cite as: AIP Advances **13**, 045301 (2023); https://doi.org/10.1063/5.0142214
Submitted: 12 January 2023 • Accepted: 13 March 2023 • Published Online: 03 April 2023

Yuan Meng, Huihui Wang, Yichi Zhang, et al.

Ultrafast charge migration in ionized iodo-alkyne chain $I(CC)_nH^+$

Cite as: AIP Advances 13, 045301 (2023); doi: 10.1063/5.0142214
Submitted: 12 January 2023 • Accepted: 13 March 2023 •
Published Online: 3 April 2023

Yuan Meng,[1] Huihui Wang,[1a)] Yichi Zhang,[2] and Yonggang Yang[1,3,b)]

AFFILIATIONS

[1] State Key Laboratory of Quantum Optics and Quantum Optics Devices, Institute of Laser Spectroscopy, Shanxi University, Taiyuan 030006, China
[2] College of Physics and Electronic Engineering, Shanxi University, Taiyuan 030006, China
[3] Collaborative Innovation Center of Extreme Optics, Shanxi University, Taiyuan 030006, China

[a)] **Author to whom correspondence should be addressed:** huihuiwang2019@sxu.edu.cn
[b)] **Electronic mail:** ygyang@sxu.edu.cn

ABSTRACT

We report ultrafast charge migration in ionized iodo-alkyne chain $I(CC)_nH^+$ for n = 1, 2, . . ., 5. The dynamics of electron density become more complicated with the increasing length of the molecular chain. However, the essential properties of charge migration in $I(CC)_nH^+$ can be clearly interpreted in terms of the electron flux. By systematic investigations of the dynamics of electron density, hole density, and the electron flux for different molecules, the size dependence of charge migration in $I(CC)_nH^+$ is discussed.

I. INTRODUCTION

Charge migration in molecules or molecular ions can be induced by ultrashort laser pulses.[1] After ionization or excitation of a molecule by one or more laser pulses, a non-equilibrium initial state that is a superposition of more than one electronic state can be prepared. The subsequent dynamics of the electron density typically represent ultrafast charge migration in the molecule.[2–10] Specifically, for the ionization of some neutral molecules, an intuitive picture of an electron hole can be used. The hole will propagate in the molecular ions. The ultrafast migration of the hole is an effect of many-electron dynamics, which has been widely studied in different molecules.[11–13] A detailed analysis of the mechanism of charge migration is very important in certain fields of photophysics and photochemistry.[1]

With the rapid development of ultrashort lasers, it becomes possible to directly detect and manipulate ultrafast processes in molecules experimentally.[14,15] The ultrafast hole migration in $ICCH^+$ with a period of 1.85 fs has been observed experimentally by Wörner and co-workers after strong field ionization of iodoacetylene.[15] In the experiment, a hole is created initially around the I atom. Subsequently, the hole migrates rapidly between the I atom and the CC triple bond. This phenomenon has been further studied theoretically to explain the results of this experiment.[16,17] Similar charge migration can be launched by ultrafast laser excitation of the $ICCH^+$ cation from its ground state.[18,19] Very recently, attosecond hole migration in halogenated hydrocarbon chains has been investigated using constrained density functional theory (DFT).[20] The speed of hole migration is found to be insensitive to the length of the molecular chain.[20]

The effects of nuclear motions are found to be important for charge migration after sufficiently long dynamics of molecules.[12,13,21–24] For example, the decoherences and recoherences of charge migration in $ICCH^+$ due to nuclear motions have been predicted theoretically.[17] The corresponding decoherence time of charge migration is about 6 fs.[17] Very recently, the phenomena of decoherences and recoherences have been observed experimentally in SiH_4.[25] The decoherence happens in the first 15 fs, and recoherence is observed in about 40–50 fs.[25] Quantitative criteria to determine the reliability of the frozen nuclei approximation for ultrafast processes have been reported based on systematic numerical simulations.[26] Accordingly, it is quite safe to use the frozen nuclei

approximation for charge migration in $ICCH^+$ for dynamics of just a few femtoseconds.

In this work, we will focus on charge migration in $I(CC)_nH^+$ $(n = 1, 2, \ldots, 5)$. The related theory and methods are provided in Sec. II. In Sec. III, we systematically investigate charge migration for the superposition of the electronic ground and first excited states of $I(CC)_nH^+$ in terms of both electron and hole dynamics. The conclusions are provided in Sec. IV.

II. THE THEORY AND METHODS

A. The electron density and hole density

The initial electronic state can be prepared as a superposition of the ground state $|\phi_0\rangle$ and the first excited state $|\phi_1\rangle$, namely, $|\psi(t=0)\rangle = c_0|\phi_0\rangle + c_1|\phi_1\rangle$, where c_0 and c_1 can be any complex numbers.[15–19] Different values of c_0 and c_1 only affect the overall amplitude of charge migration and do not change the essential properties.[16] For simplicity, we chose $c_0 = c_1 = \frac{1}{\sqrt{2}}$. The subsequent time-dependent state can be obtained according to the solution of the Schrödinger equation

$$|\psi(t)\rangle = \frac{\sqrt{2}}{2}(|\phi_0\rangle + |\phi_1\rangle e^{-i\omega t}), \tag{1}$$

where $\omega = \Delta E/\hbar$ and ΔE is the excitation energy from $|\phi_0\rangle$ to $|\phi_1\rangle$.

The electron density can be evaluated as the mean value of the density operator,

$$\rho(\mathbf{r}, t) = \langle\psi(t)|\hat{\rho}(\mathbf{r})|\psi(t)\rangle. \tag{2}$$

Here, the density operator is

$$\hat{\rho}(\mathbf{r}) = \sum_{k=1}^{N_{el}} \delta(\mathbf{r} - \mathbf{r}_k), \tag{3}$$

where $\mathbf{r}_k$ is the spatial coordinate of the k-th electron.

To continue the numerical calculations, we will need the elements $\rho_{ij}(\mathbf{r}) = \langle\phi_i|\hat{\rho}(\mathbf{r})|\phi_j\rangle$. They are calculated using ORBKIT as implemented by Tremblay and co-workers.[27–29] The required many-electron wavefunctions of $|\phi_0\rangle$ and $|\phi_1\rangle$ are obtained using the state-averaged complete active space self-consistent field (CASSCF) method as implemented in MOLPRO.[30] The basis set is cc-pVTZ for H,C and cc-pVTZ-PP for I, which will be called cc-pVTZ* in the following.

According to previous experimental and theoretical investigations of charge migration in $ICCH^+$, it is sufficient to focus on charge migration along the molecular axis. We define the coordinate frame such that all the molecules are along the z-axis. The one-dimensional electron density along the molecular axis can be obtained by integration of $\rho(\mathbf{r}, t)$ over x and y,

$$\rho(z, t) = \iint \rho(\mathbf{r}, t)dxdy. \tag{4}$$

The value of $\rho(z, t)$ is typically very large for z close to the position of an atom, which makes it difficult to visualize the dynamics of $\rho(z, t)$. A convenient way is to define the fluctuation part of the density as

$$\Delta\rho(z, t) = \rho(z, t) - \rho(z, t = 0). \tag{5}$$

Apparently, the dynamics of $\rho(z, t)$ are equivalent to the dynamics of $\Delta\rho(z, t)$.

In the literature, it is often helpful to define a pseudo-particle called an electron hole.[31–34] In this way, the dynamics of N-electrons can be simplified to the dynamics of one particle. The hole density $\rho_h(z, t)$ is defined as the difference between the electron density of the neutral molecule and that of the corresponding cation,

$$\rho_h(z, t) = \rho^{neu}(z) - \rho(z, t), \tag{6}$$

where $\rho(z, t)$ is defined in Eq. (4) and $\rho^{neu}(z)$ is the one-dimensional electron density of the neutral molecule along the z-axis. The density $\rho^{neu}(z)$ is calculated at the same level of theory as that of $\rho(z, t)$ for the neutral molecule in the electronic ground state. The definition of the hole density in Eq. (6) is consistent with previous work in Refs. 31–34.

B. Characterization of charge migration

Apart from the electron density and the hole density, a more convenient quantity to characterize charge migration is the electron flux. According to the one-dimensional continuity equation, the electron flux $F_z(z, t)$ along the molecular axis can be evaluated as

$$F_z(z, t) = -\int_{z_0}^{z} \frac{\partial\Delta\rho(z', t)}{\partial t} dz'. \tag{7}$$

Equation (7) is integrated numerically. The position of z_0 should be sufficiently far away from the molecule such that the electron flux at $z = z_0$ is always zero. For each of the investigated molecules, the corresponding center of mass is the origin of the coordinate frame. The z coordinate of the hydrogen atom of each molecule is negative. The value of z_0 is chosen to be $5a_0$ smaller than the corresponding z coordinate of the hydrogen atom.

The direct effect of charge migration is the variation of the dipole moments. The time-dependent dipole moment of the system can be obtained by evaluating the mean value of the dipole operator for any given time,

$$\mathbf{d}(t) = -\langle\psi(t)|\hat{\mathbf{d}}|\psi(t)\rangle, \tag{8}$$

where the dipole operator is

$$\hat{\mathbf{d}} = -\sum_{k=1}^{N_{el}} e\mathbf{r}_k + \sum_{i=1}^{N_{nuc}} Q_i\mathbf{R}_i, \tag{9}$$

here, Q_i and $\mathbf{R}_i$ are the nuclear charge and nuclear coordinate of the ith nucleus, respectively.

In this work, only the z-component of $\mathbf{d}(t)$ is nonzero. It can be calculated according to Eq. (8) as

$$\begin{aligned} d_z(t) &= \hat{\mathbf{e}}_z \cdot \mathbf{d}(t), \\ &= -e\int_{-\infty}^{+\infty} z\rho(z, t)dz + \sum_{i=1}^{N_{nuc}} Q_i(\hat{\mathbf{e}}_z \cdot \mathbf{R}_i), \end{aligned} \tag{10}$$

where $\hat{\mathbf{e}}_z$ is the unit vector along the z-axis. According to Eq. (6), we can obtain the following relation:

$$d_z(t) = e\langle z_h(t)\rangle + d_z^{neu}, \tag{11}$$

where $\langle z_h(t)\rangle$ is the mean position of the hole

$$\langle z_h(t)\rangle = \int_{-\infty}^{+\infty} z\rho_h(z,t)dz. \tag{12}$$

Here $\mathbf{d}^{neu}$ is the dipole moment of the neutral molecule. The only non-zero component of $\mathbf{d}^{neu}$ is the z-component d_z^{neu}.

III. RESULTS AND DISCUSSION

A. Charge migration in $I(CC)_nH^+$

The frozen nuclei approximation has been widely used in the investigations of charge migration. There are two facts to validate this approximation. First, the time scale of charge migration is typically less than 10 fs, and the corresponding effects of nuclear motions are negligible in most cases. Second, the essential properties of charge migration are rather robust for different molecular geometries with relatively small differences. We will only focus on charge migration in a few fs. Therefore, the molecular structures can be assumed to be frozen.

In the literature, there are typically two different choices of molecular structures that lead to similar phenomena of charge migration. The first scenario is the strong field ionization of neutral molecules. The corresponding $I(CC)_nH^+$ cations can be prepared in the superposition state in Eq. (1) after ionization. In this case, the structures of $I(CC)_nH^+$ are assumed to be the same as the corresponding neutral molecules. The second scenario is to excite the ground-state cations directly using ultrashort laser pulses. In this case, the structures of $I(CC)_nH^+$ are assumed to be the same as the equilibrium structures of the cations in their electronic ground states. For the subsequent simulations, we consider the first scenario. Namely, the structures of $I(CC)_nH^+$ are frozen at the equilibrium structures of the corresponding neutral molecules. Accordingly, the structures of the neutral molecules are optimized at the same level of theory, which is CASSCF/cc-pVTZ*, using MOLPRO.

Charge migration will occur periodically for frozen nuclei. The period T can be calculated according to the first excitation energy ΔE as $T = h/\Delta E$. Accordingly, the values of ΔE and T for different cations $I(CC)_nH^+$ ($n = 1, 2, \ldots, 5$) are documented in Table I. The active spaces in CASSCF calculations for different cations are carefully chosen based on the experiences of previous work.[16–19] The number of unoccupied active orbitals is the same for all the $I(CC)_nH^+$ cations. While the occupied orbitals are included as needed. The active spaces of $I(CC)_nH^+$ are also provided in the last row of Table I. We further calculate ΔE of each cation, including spin–orbit couplings. The corresponding correction to each ΔE is only a few percent.

TABLE I. The first excitation energy ΔE and the corresponding period T of charge migration for each $I(CC)_nH^+$ cation. The active space for CASSCF is also listed.

n	1	2	3	4	5
ΔE (eV)	2.20	1.83	1.75	1.65	1.45
T (fs)	1.88	2.26	2.36	2.50	2.86
Active space	(12,15)	(15,21)	(14,19)	(12,15)	(14,19)

The first excited state of each $I(CC)_nH^+$ is a $\pi\pi^*$ excitation, with an increasing number of carbon atoms participating in the $\pi\pi$ interaction as n increases. Consequently, we find a systematic decrease of the first excitation energy ΔE of $I(CC)_nH^+$ for increasing n. Specifically, ΔE decreases from 2.2 eV for $ICCH^+$ to 1.45 eV for $I(CC)_5H^+$. The corresponding period T of charge migration increases from about 1.9 fs for $ICCH^+$ to 2.9 fs for $I(CC)_5H^+$. The details of charge migration are shown in Fig. 1 for different $I(CC)_nH^+$ cations.

The ultrafast electron dynamics of $I(CC)_nH^+$ ($n = 1, 2, \ldots, 5$) are illustrated in Figs. 1(a)–1(e), respectively, by contour plots for the fluctuation part of electron density $\Delta\rho_{el}(z,t)$ in Eq. (5) for $t < 3$ fs. For all the panels of Fig. 1, the vertical axes are the z coordinates with the same scale for different cations, and the red and blue colors represent positive and negative contour values, respectively. Note that the specific contour values of different panels are different for better visualization of all the panels. For precise numbers, the maximum and minimum values of $\Delta\rho_{el}(z,t)$ and the electron flux $F_z(z,t)$ of Figs. 1(a)–1(j) are provided in Table II.

Specifically, Fig. 1(a) shows the spatiotemporal dynamics of $\Delta\rho_{el}(z,t)$ of $ICCH^+$. As can be seen, the electron density around the I atom increases in the first half period and decreases in the second half period. While the electron density around the C≡C triple bond first decreases and then increases during the same period. We can, therefore, clearly identify charge migration from the region around the C≡C triple bond to the region around the I atom and back in one period. The results agree with previous investigations.[16,17] Charge migration in $ICCH^+$ can be easily identified from Fig. 1(f) for the electron flux $F_z(z,t)$ along the z-axis. The value of $|F_z(z,t)|$ is significantly larger than zero only in the region between the C≡C triple bond and the I atom, which means charge migration occurs mainly in this region. In addition, $F_z(z,t)$ in this region is positive for the first half period and negative for the second half period. This illustrates the same electron dynamics as in Fig. 1(a), but in a clearer representation.

When the length of $I(CC)_nH^+$ increases, namely the value of n increases, the dynamics of the electron density become more complicated. The corresponding dynamics of $\Delta\rho_{el}(z,t)$ of $I(CC)_2H^+$ in Fig. 1(b) has some properties similar to those of $ICCH^+$ in Fig. 1(a). The electron density around the I atom also first increases and then decreases in the first period. There is more than one C≡C triple bond. In the following, we will refer to the C≡C nearest to the I atom as the first C≡C triple bond, and the next ones are the second, third, and so on. The electron density around the second C≡C triple bond first decreases and then increases in the first period, which is similar to that of $ICCH^+$. While the region around the first C≡C triple bond contains two regions with opposite electron density fluctuations, it becomes difficult to find the direction of charge migration in this region only according to the properties of $\Delta\rho_{el}(z,t)$.

However, the essential properties of charge migration of $I(CC)_2H^+$ can be clearly identified from the electron flux $F_z(z,t)$ in Fig. 1(g). Accordingly, charge migration is unidirectional in the first half period in any region of the molecule. The direction of the charge migration is along the positive direction of the z-axis, namely, from the H atom pointing to the I atom. The electron flux is different from zero mainly in two regions: from the first C≡C triple bond to the I atom, and from the second to the first C≡C triple bond. For the next half period, the electron flux is still unidirectional but

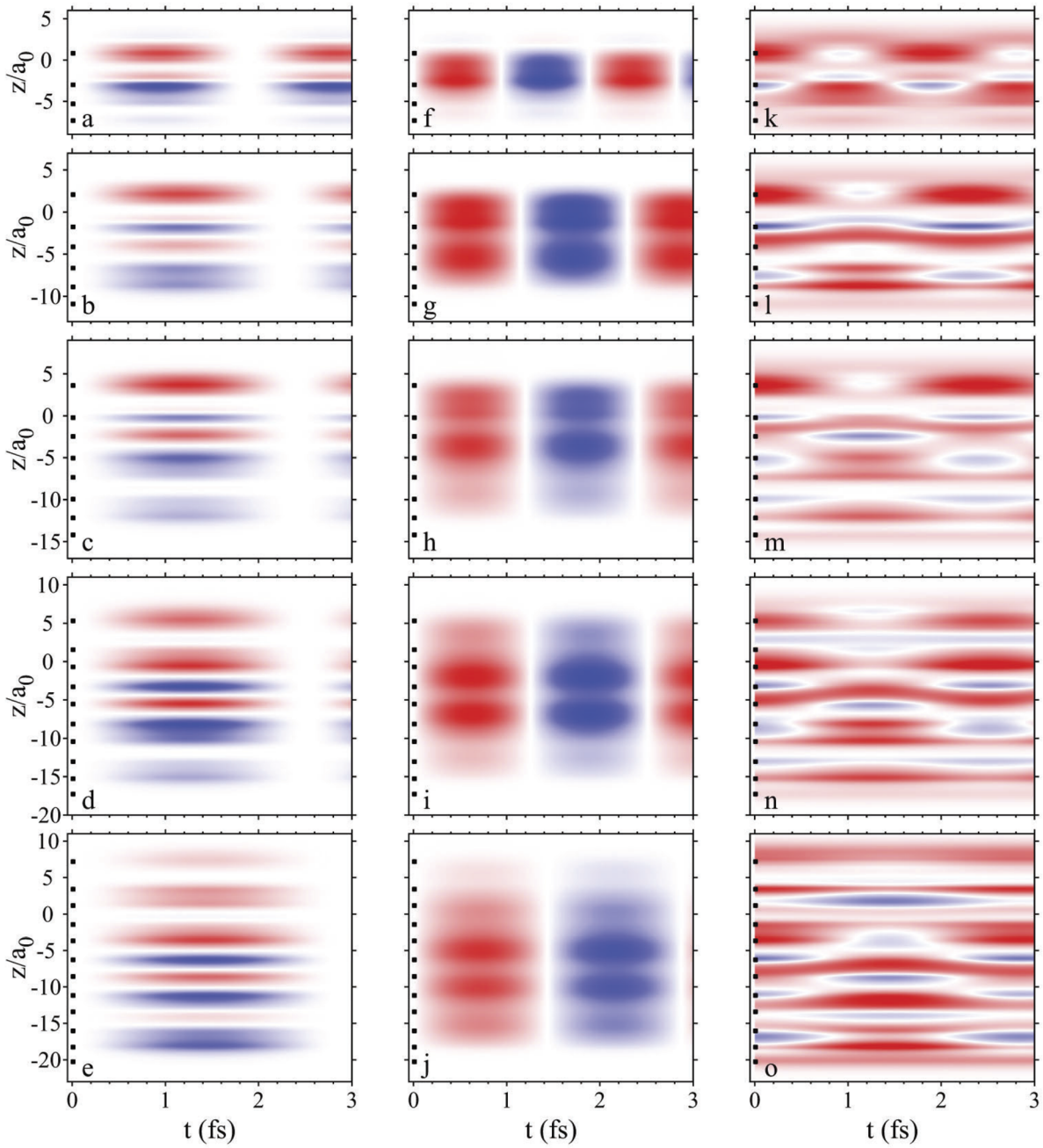

FIG. 1. Charge migration of $I(CC)_nH^+$ along the molecular axis (z-axis) for the first 3 fs with color-coded contour plots. The $I(CC)_nH^+$ cations are in the superposition of the electronic ground and first excited states. (a)–(e) The fluctuation part of the electron density $\Delta\rho_{el}(z,t)$ in the center of mass coordinate frame of $I(CC)_nH^+$, for $n = 1, 2, \ldots, 5$ from top to bottom. (f)–(j) Same as (a)–(e), but for the electron flux $F_z(z,t)$ of $I(CC)_nH^+$ along the z-axis. (k)–(o) Same as (a)–(e), but for the propagation of the hole density $\rho_h(z,t)$ in Eq. (6). For each panel (a)–(o), the position of each atom is indicated as a small black dot on the left, where the top atom is I and the bottom atom is H.

changes its direction, namely, pointing to the negative part of the z-axis.

Concerning the fluctuations of electron density $\Delta\rho_{el}(z,t)$ of $I(CC)_nH^+$ $(n = 3, 4, 5)$ shown in Figs. 1(c)–1(e), there are some systematic characteristics. The electron density around the last two C≡C triple bonds decreases in the first half period and increases in the next half period. While the region around the last third C≡C triple bonds of each cation in Figs. 1(c)–1(e) splits into two

TABLE II. The maximum and minimum values of $\Delta\rho_{el}(z,t)/a_0^{-1}$ and $F_z(z,t)/fs^{-1}$ for charge migration in $I(CC)_nH^+$ shown in Figs. 1(a)–1(j).

n	1	2	3	4	5
Max $\Delta\rho_{el}(z,t)$	0.305	0.301	0.265	0.175	0.155
Min $\Delta\rho_{el}(z,t)$	−0.334	−0.210	−0.184	−0.187	−0.159
Max/min $F_z(z,t)$	±0.024	±0.020	±0.021	±0.020	±0.017

regions in which the electron density fluctuates oppositely. For sufficiently long cations, the electron density around the first one or more C≡C triple bonds first increases and then decreases in the first half period. For all the investigated cations, $I(CC)_nH^+$ ($n = 1,2,\ldots,5$), the electron dynamics around the I atom are essentially the same, but the amplitudes of charge migration decrease when n increases.

The behaviors of charge migration in all the $I(CC)_nH^+$ ($n = 1,2,\ldots,5$) can be clearly characterized in terms of the electron flux $F_z(z,t)$, irrespective of the corresponding complicated dynamics of $\Delta\rho_{el}(z,t)$ in Figs. 1(a)–1(e). Accordingly, all the charge migrations of $I(CC)_nH^+$ are unidirectional in the first half period. The electron fluxes are nonzero mainly in the regions from the first C≡C triple bond to the I atom and from the nth to the $(n-1)$th C≡C triple bonds. For the next half period, the corresponding charge migrates back to the initial positions. Apparently, when the cation becomes longer, the region of charge migration increases. However, the average amplitude of charge migration decreases when n increases so that the total number of migrating electrons is more or less the same for different cations.

The same electron dynamics can also be represented with an electron hole. Accordingly, the hole densities $\rho_h(z,t)$ of $I(CC)_nH^+$ ($n = 1,2,\ldots,5$) are shown in Figs. 1(k)–1(o). The advantage of the electron hole is that we can see particle-like motions. For each of the cations $I(CC)_nH^+$, the hole migrates from the region around the I atom to the region of the first C≡C triple bond for the first half period and migrates back in the next half period. For relatively long cations, we can also identify hole migration from the last second to the last C≡C triple bond. However, it is very difficult to identify even the direction of hole migration in some central regions of relevant $I(CC)_nH^+$ cations. This is not strange since the dynamics of the hole are almost the opposite counterpart of the electron dynamics represented by $\Delta\rho_{el}(z,t)$. Note that there are some special values of z for which $\Delta\rho_{el}(z,t)$ is always zero. This does not imply stationary points. On the contrary, such points have maximum electron flux $F_z(z,t)$. The reason $\Delta\rho_{el}(z,t) = 0$ is that electrons flow into and out of such points at rates equal to each other. The corresponding dynamics of the electrons or the hole can only be clearly unraveled in terms of the electron flux $F_z(z,t)$. Accordingly, the best tool for transparent representations of charge migration is the electron flux $F_z(z,t)$ shown in Figs. 1(f)–1(j).

B. Transient molecular properties due to charge migration

Charge migration will affect certain molecular properties. The most important one is the dipole moment. Due to charge migration, the molecular dipole oscillates accordingly. The only nonzero component of the dipole, which is $d_z(t)$ in Eq. (10), is shown in Fig. 2(b) for each cation. The corresponding period of the dipole oscillations of $I(CC)_nH^+$ is the same as the values in Table I. The amplitude of the dipole oscillation of $I(CC)_nH^+$ increases as n increases. This is consistent with the properties of charge migration in Fig. 1. Namely, the range of charge migration increases with increasing cation length, while the total number of migrating electrons is more or less the same for different cations. The values of the dipole moments decrease in the first half period and increase in the second half period. This is also consistent with Fig. 1. For an easy comparison, see Figs. 1(f)–1(j) for the directions of charge migration.

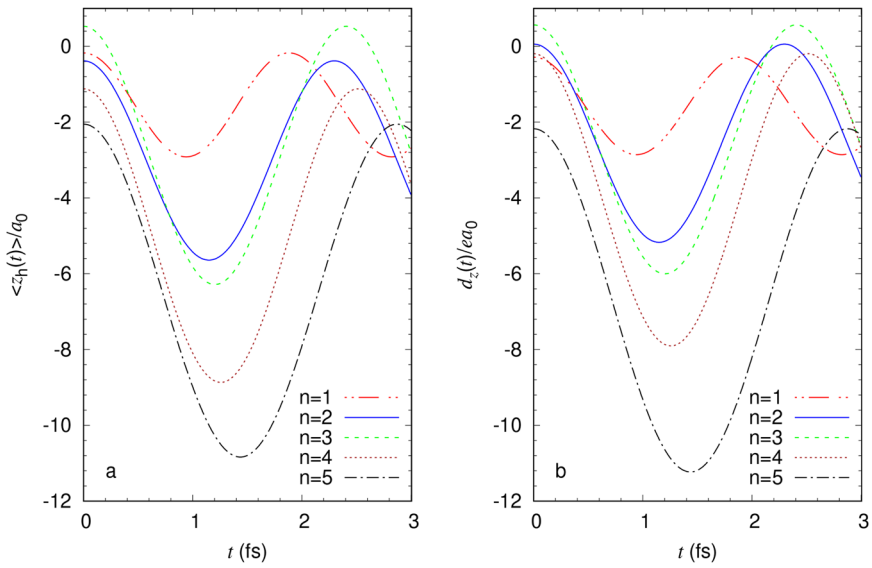

FIG. 2. The time-dependent mean value of the position of (a) the hole $\langle z_h(t)\rangle$ and (b) the dipole moment $d_z(t)$ of $I(CC)_nH^+$ ($n = 1,2,\ldots,5$).

The dipole moments of $I(CC)_nH^+$ can also be evaluated in terms of the hole density $\rho_h(z,t)$, which is given in Eqs. (11) and (12). This severs as a good method to check the reliability of the intuitive picture of a hole. Accordingly, Fig. 2(a) shows the dynamics of the mean position of the hole, namely $\langle z_h(t)\rangle$ in Eq. (12), for each $I(CC)_nH^+$ cation. Similarly, the mean position of the hole of each cation oscillates periodically, with the same period as in Table I. The velocity of the hole migration can also be estimated according to the slope of each curve in Fig. 2(a), leading to similar results as have been reported in Ref. 20. Namely, the migration velocity of the hole is not sensitive to the length of the chain. According to Eq. (12), the only difference between $d_z(t)$ and $e\langle z_h(t)\rangle$ of each $I(CC)_nH^+$ cation is the permanent dipole moment of the neutral $I(CC)_nH$ molecule. Consequently, the differences between the corresponding curves in Figs. 2(a) and 2(b) are purely certain constants. All the neutral $I(CC)_nH$ molecules have nonzero dipole moments along the z-axis. However, the values of the permanent dipole moments are all very small compared to the amplitudes of the oscillations in Fig. 2(b). Therefore, the curves in Figs. 2(a) and 2(b) are almost the same.

IV. CONCLUSIONS

In summary, we have systemically investigated charge migration in $I(CC)_nH^+$ cations with frozen nuclei approximation. Charge migrations are found to be unidirectional, irrespective of the complicated electron or hole dynamics of different cations. Specifically, an electron hole is created after strong field ionization of the corresponding neutral molecules. Subsequently, the hole migrates along the molecular axis periodically. For the first half period, the hole migrates unidirectionally along the direction pointing from the I to the H atoms. For the second half period, the hole migrates back to the initial positions.

When the size of the $I(CC)_nH^+$ cation increases, the corresponding hole dynamics become more and more intricate. For $I(CC)H^+$, the hole is located around the I atom initially. For longer cations, the hole is located not only around the I atom but also in the regions of one or more C≡C triple bonds close to the I atom. Both the periods and ranges of charge migration increase when the lengths of the cations increase. While the total number of migrating electrons is more or less the same for different $I(CC)_nH^+$ cations. This can be understood in terms of the electron hole. The total number of migrating hole is more or less one for different cations.

The present work focuses on the short time electron dynamics of only 3 fs. For long time dynamics, the effects of nuclear motions are important. The decoherence of charge migration will happen, and it will be interesting to investigate how the decoherence time depends on the molecular size. This is beyond the scope of the present work and will be studied separately. The results of the present work should provide a helpful reference for future investigations of size-dependent charge migration in molecular systems.

ACKNOWLEDGMENTS

This work was supported by the National Key Research and Development Program of China under Grant No. 2017YFA0304203, the Program for Changjiang Scholars and Innovative Research Team under Grant No. IRT_17R70, the National Natural Science Foundation of China under Grant No. 11904215, the Fundamental Research Program of Shanxi Province under Grant No. 202203021211301, the 111 Project under Grant No. D18001, the Fund for Shanxi 1331 Project Key Subjects Construction, and the Hundred Talent Program of Shanxi Province.

AUTHOR DECLARATIONS

Conflict of Interest

There are no conflicts of interest to declare.

Author Contributions

Yuan Meng: Data curation (equal); Formal analysis (equal). **HuiHui Wang**: Data curation (equal); Funding acquisition (equal); Supervision (equal); Validation (equal); Writing – review & editing (equal). **Yichi Zhang**: Funding acquisition (equal); Writing – review & editing (equal). **Yonggang Yang**: Conceptualization (equal); Methodology (equal); Supervision (equal); Writing – original draft (equal); Writing – review & editing (equal).

DATA AVAILABILITY

The data that support the findings of this study are available within the article.

REFERENCES

[1]H. J. Wörner, C. A. Arrell, N. Banerji, A. Cannizzo, M. Chergui, A. K. Das, P. Hamm, U. Keller, P. M. Kraus, E. Liberatore, P. Lopez-Tarifa, M. Lucchini, M. Meuwly, C. Milne, J.-E. Moser, U. Rothlisberger, G. Smolentsev, J. Teuscher, J. A. van Bokhoven, and O. Wenger, "Charge migration and charge transfer in molecular systems," Struct. Dyn. **4**, 061508 (2017).

[2]R. Weinkauf, P. Schanen, D. Yang, S. Soukara, and E. W. Schlag, "Elementary processes in peptides: Electron mobility and dissociation in peptide cations in the gas phase," J. Phys. Chem. **99**, 11255 (1995).

[3]F. Remacle, R. D. Levine, E. W. Schlag, and R. Weinkauf, "Electronic control of site selective reactivity: A model combining charge migration and dissociation," J. Phys. Chem. A **103**, 10149 (1999).

[4]I. Barth and J. Manz, "Periodic electron circulation induced by circularly polarized laser pulses: Quantum model simulations for Mg porphyrin," Angew. Chem., Int. Ed. **45**, 2962 (2006).

[5]M. Kanno, H. Kono, and Y. Fujimura, "Control of π-electron rotation in chiral aromatic molecules by nonhelical laser pulses," Angew. Chem., Int. Ed. **45**, 7995 (2006).

[6]S. Chelkowski, G. L. Yudin, and A. D. Bandrauk, "Observing electron motion in molecules," J. Phys. B: At., Mol. Opt. Phys. **39**, S409 (2006).

[7]I. Barth, J. Manz, Y. Shigeta, and K. Yagi, "Unidirectional electronic ring current driven by a few cycle circularly polarized laser pulse: Quantum model simulations for Mg-porphyrin," J. Am. Chem. Soc. **128**, 7043 (2006).

[8]F. Remacle, M. Nest, and R. D. Levine, "Laser steered ultrafast quantum dynamics of electrons in LiH," Phys. Rev. Lett. **99**, 183902 (2007).

[9]I. S. Ulusoy and M. Nest, "Correlated electron dynamics: How aromaticity can be controlled," J. Am. Chem. Soc. **133**, 20230 (2011).

[10]G. Hermann, V. Pohl, G. Dixit, and J. C. Tremblay, "Probing electronic fluxes via time-resolved X-ray scattering," Phys. Rev. Lett. **124**, 013002 (2020).

[11]L. S. Cederbaum and J. Zobeley, "Ultrafast charge migration by electron correlation," Chem. Phys. Lett. **307**, 205 (1999).
[12]Z. Li, O. Vendrell, and R. Santra, "Ultrafast charge transfer of a valence double hole in glycine driven exclusively by nuclear motion," Phys. Rev. Lett. **115**, 143002 (2015).
[13]V. Despré, N. V. Golubev, and A. I. Kuleff, "Charge migration in propiolic acid: A full quantum dynamical study," Phys. Rev. Lett. **121**, 203002 (2018).
[14]F. Calegari, D. Ayuso, A. Trabattoni, L. Belshaw, S. De Camillis, S. Anumula, F. Frassetto, L. Poletto, A. Palacios, P. Decleva, J. B. Greenwood, F. Martín, and M. Nisoli, "Ultrafast electron dynamics in phenylalanine initiated by attosecond pulses," Science **346**, 336–339 (2014).
[15]P. M. Kraus, B. Mignolet, D. Baykusheva, A. Rupenyan, L. Horný, E. F. Penka, G. Grassi, O. I. Tolstikhin, J. Schneider, F. Jensen, L. B. Madsen, A. D. Bandrauk, F. Remacle, and H. J. Wörner, "Measurement and laser control of attosecond charge migration in ionized iodoacetylene," Science **350**, 790 (2015).
[16]H. Ding, D. Jia, J. Manz, and Y. Yang, "Reconstruction of the electronic flux during adiabatic attosecond charge migration in $HCCI^+$," Mol. Phys **115**, 1813–1825 (2017).
[17]D. Jia, J. Manz, and Y. Yang, "De-and recoherence of charge migration in ionized iodoacetylene," J. Phys. Chem. Lett. **10**, 4273–4277 (2019).
[18]D. Jia, J. Manz, and Y. Yang, "Timing the recoherences of attosecond electronic charge migration by quantum control of femtosecond nuclear dynamics: A case study for $HCCI^+$," J. Chem. Phys. **151**, 244306 (2019).
[19]D. Jia, J. Manz, and Y. Yang, "Generation of electronic flux during the femtosecond laser pulse tailored to induce adiabatic attosecond charge migration in $HCCI^+$," J. Mod. Opt. **64**, 960–970 (2017).
[20]A. S. Folorunso, A. Bruner, F. Mauger, K. A. Hamer, S. Hernandez, R. R. Jones, L. F. DiMauro, M. B. Gaarde, K. J. Schafer, and K. Lopata, "Molecular modes of attosecond charge migration," Phys. Rev. Lett. **126**, 133002 (2021).
[21]A. D. Bandrauk, S. Chelkowski, P. B. Corkum, J. Manz, and G. L. Yudin, "Attosecond photoionization of a coherent superposition of bound and dissociative molecular states: Effect of nuclear motion," J. Phys. B: At., Mol. Opt. Phys. **42**, 134001 (2009).
[22]V. Despré, A. Marciniak, V. Loriot, M. C. E. Galbraith, A. Rouzée, M. J. J. Vrakking, F. Lépine, and A. I. Kuleff, "Attosecond hole migration in Benzene molecules surviving nuclear motion," J. Phys. Chem. Lett. **6**, 426 (2015).
[23]A. Nikodem, R. D. Levine, and F. Remacle, "Quantum nuclear dynamics pumped and probed by ultrafast polarization controlled steering of a coherent electronic state in LiH," J. Phys. Chem. A **120**, 3343 (2016).
[24]C. Arnold, O. Vendrell, and R. Santra, "Electronic decoherence following photoionization: Full quantum-dynamical treatment of the influence of nuclear motion," Phys. Rev. A **95**, 033425 (2017).
[25]D. T. Matselyukh, V. Despré, N. V. Golubev, A. I. Kuleff, and H. J. Wörner, "Decoherence and revival in attosecond charge migration driven by non-adiabatic dynamics," Nat. Phys. **18**, 1206 (2022).
[26]D. Jia and Y. Yang, "Systematic investigation of the reliability of the frozen nuclei approximation for short-pulse excitation: The example of $HCCI^+$," Front. Chem. **10**, 857348 (2022).
[27]G. Hermann, V. Pohl, J. C. Tremblay, B. Paulus, H.-C. Hege, and A. Schild, "ORBKIT: A modular python toolbox for cross-platform postprocessing of quantum chemical wavefunction data," J. Comput. Chem. **37**, 1511 (2016).
[28]G. Hermann, V. Pohl, and J. C. Tremblay, "An open-source framework for analyzing *N*-electron dynamics. II. hybrid density functional theory/configuration interaction methodology," J. Comput. Chem. **38**, 2378 (2017).
[29]V. Pohl, G. Hermann, and J. C. Tremblay, "An open-source framework for analyzing n-electron dynamics. I. multideterminantal wave functions," Chem. Phys. **38**, 1515 (2017).
[30]H. J. Werner, P. J. Knowles, G. Knizia *et al.*, MOLPRO, version 2012.1, a package of *ab initio* programs, 2012, see http://www.molpro.net.
[31]J. Breidbach and L. S. Cederbaum, "Migration of holes: Formalism, mechanisms, and illustrative applications," J. Chem. Phys. **118**, 3983 (2003).
[32]A. I. Kuleff, J. Breidbach, and L. S. Cederbaum, "Multielectron wave-packet propagation: General theory and application," J. Chem. Phys. **123**, 044111 (2005).
[33]V. Despré and A. I. Kuleff, "Correlation-driven charge migration as an initial step of the dynamics in correlation bands," Phys. Rev. A **106**, L021501 (2022).
[34]V. Kochetov and S. I. Bokarev, "RhoDyn: A ρ-TD-RASCI framework to study ultrafast electron dynamics in molecules," J. Chem. Theory Comput. **18**, 46 (2022).